Biosensors and Bioelectronics 56 (2014) 345–351

Contents lists available at ScienceDirect

Biosensors and Bioelectronics

journal homepage: www.elsevier.com/locate/bios

Disposable amperometric biosensor based on lactate oxidase immobilised on platinum nanoparticle-decorated carbon nanofiber and poly(diallyldimethylammonium chloride) films

Pedro J. Lamas-Ardisana [a,*], Oscar A. Loaiza [a], Larraitz Añorga [a], Elena Jubete [a], Maryam Borghei [b], Virginia Ruiz [a], Estibalitz Ochoteco [a], Germán Cabañero [a], Hans J. Grande [a]

[a] Sensors Unit, Materials Division, IK4-CIDETEC, Parque Tecnológico de San Sebastián, Paseo Miramón 196, 20009 Donostia-San Sebastián, Spain
[b] Department of Applied Physics, Aalto University School of Science, P.O. Box 15100, 00076 Aalto, Finland

ARTICLE INFO

Article history:
Received 3 December 2013
Received in revised form
22 January 2014
Accepted 23 January 2014
Available online 31 January 2014

Keywords:
Lactate
Lactate oxidase
Screen-printed electrode
Carbon nanofiber
Platinum nanoparticle
Sweat

ABSTRACT

A novel biosensor for lactate has been developed, using screen-printed carbon electrodes (SPCE) and lactate oxidase (LOx). The active surface of the electrodes was modified using a dispersion of platinum nanoparticle decorated carbon nanofibers (PtNp-CNF) in poly(diallyldimethylammonium) chloride (PDDA) solution. In this way, sensitive, disposable, low cost and reliable hydrogen peroxide sensors were obtained. The immobilisation of LOx on top of these PtNp-CNF-PDDA/SPCEs resulted in amperometric biosensors with high operational stability. The sensitivity of the optimised lactate biosensor was 36.8 (mA/M cm^2) with a linear range of 25–1500 μM. The limit of detection was 11 μM ($S/N=3$). Reproducibility, selectivity and storage stability were also evaluated. Additionally, the stability of the biosensor was also predicted by a model based on thermal degradation. Finally, lactate in sweat and blood samples was determined in a sport test using LOx/PtNp-CNF-PDDA/SPCEs and commercial biosensors respectively. Based on these data, the validity of the sweat lactate for the determination of the lactate threshold is discussed.

1. Introduction

Lactate is the key metabolite of the anaerobic glycolytic pathway. Lactate concentration in blood is an excellent indirect marker of anaerobic glucose breakdown, and so, cellular fatigue. Development of reliable methods of lactate determination is of great importance in clinical analysis because the concentration of lactate in blood is a fundamental parameter for the prevention and diagnosis of a number of pathological disorders such as hypoxia (Artiss et al., 2000; Frost and Meyerhoff, 2006), some acute heart diseases and drug toxicity (Pfeiffer et al., 1997; Przybyt et al., 2010). Lactate monitoring is also important in sport medicine because it is used to evaluate the maximum performance of an athlete in intensive and endurance-based activities. In this case, the physical condition is directly related to the lactate threshold i.e. the maximum steady state effort that can be maintained without increase in blood lactate (Faude et al., 2009).

Different techniques have been used for the determination of blood lactate such as HPLC (Simonides et al., 1988), enzymatic colorimetric assays (Saunders et al., 2005) or portable analysers (Buckley et al., 2003). Latest ones, based on finger-stick blood sampling and disposable sensor strips, could be considered the most adequate to obtain real temporal lactate profiles during physical training (Andrzejewski et al., 2012; Faridnia et al., 1993; Guilbault et al., 1995). However an inherent drawback of this methodology is the intrusiveness and inconvenience in the exercise routines. Hence researchers have indeed made efforts in order to develop non-invasive methods and new designs have been proposed such as lactate biosensors in a contact lens (Thomas et al., 2012) or in tattoos (Jia et al., 2013). The latest is connected with the concentration of lactate in sweat which has been proposed to evaluate the exercise intensity and the fitness level. Perspiration may thus be conveniently utilised for the analysis of physical performance in individuals without the need for an invasive blood sampling approach (Faridnia et al., 1993; Guilbault et al., 1995). Nevertheless, there is controversy over the validity of this parameter in sport training methods (Derbyshire et al., 2012). On the other hand, sweat lactate can also serve as a sensitive marker of tissue viability and may provide warning for pressure

* Corresponding author. Tel.: +34 943309022; fax: +34 943309136.
E-mail address: plamas@cidetec.es (P.J. Lamas-Ardisana).

0956-5663/$ - see front matter © 2014 Elsevier B.V. All rights reserved.
http://dx.doi.org/10.1016/j.bios.2014.01.047

ischaemia, reflecting the insufficient oxidative metabolism and a compromise of tissue viability (Polliack et al., 1997).

Several amperometric lactate biosensors based on screen-printing have been previously reported (Albareda-Sirvent and Hart, 2002; Collier et al., 1996; Perez and Fabregas, 2012; Perez et al., 2012; Piano et al., 2010; Rawson et al., 2009; Shimomura et al., 2012). This technology has been successfully employed for the fabrication of electrodes in the last decade, allowing mass production of disposable low-cost sensors (Avramescu et al., 2002; Fanjul-Bolado et al., 2008; Tudorache and Bala, 2007). Lactate dehydrogenases (Piano et al., 2010) or lactate oxidases (LOx) (Albareda-Sirvent and Hart, 2002; Collier et al., 1996; Perez and Fabregas, 2012; Perez et al., 2012; Rawson et al., 2009; Shimomura et al., 2012) are immobilised on these electrode surfaces in order to obtain biosensors. LOx, the enzyme most widely used for lactate biosensors, catalyses the conversion of lactate to pyruvate and H_2O_2, which is subsequently detected by amperometry. This detection is limited in analytical applications by slow electrode kinetics and high overpotentials which may cause large interferences from other electroactive species in real samples. Therefore the current research on H_2O_2 detection is mainly focused on electrode modifications in order to overcome the limitations above mentioned (Chen et al., 2012). In this regard, nanomaterials have attracted tremendous interest in biosensor research. Some of them have shown great advantages over conventional materials for H_2O_2 detection such as ZnO nanorod arrays (Wang et al., 2011), MnO_2-modified vertically aligned multiwalled carbon nanotubes (Xu et al., 2010a), nitrogen-doped carbon nanotubes (Xu et al., 2010b) or platinum nanoparticles (PtNp) (Chikae et al., 2006). Carbon nanomaterials, especially carbon nanotubes and carbon nanofibers (CNFs), have also attracted considerable attention in H_2O_2 detection (Fanjul-Bolado et al., 2007; Wang et al., 2003). Carbon nanotubes are more used than CNFs, however the utility of the CNFs in biosensors has been recently reviewed (Huang et al., 2010). On the other hand, a new trend in biosensor design is the combination of two or more nanomaterials i.e. hybrid nanomaterials (Xiao and Li, 2008). In this sense, carbon nanotubes decorated with PtNp have been recently exploited (Huang et al., 2008; Male et al., 2007). CNFs decorated with PtNp (PtNp-CNF) are more extensively studied in fuel-cell research (Andersen et al., 2013; Wang et al., 2012). Nevertheless, these nanohybrid materials have been recently used for H_2O_2 detection and their applications in biosensor have been proposed (Liu et al., 2011).

In this work, a novel biosensor for lactate was developed, using screen-printed carbon electrodes (SPCE) and LOx. PtNp-CNFs were obtained by the polyol method and dispersed in poly(diallyldimethylammonium) chloride (PDDA) solution. The modification of SPCEs was optimised for H_2O_2 detection. Then, the LOx was immobilized on top of these PtNp-CNF-PDDA/SPCEs. The resulting biosensor was characterised and sensitivity, linear range, limit of detection, reproducibility, selectivity and storage stability were determined. Finally, the biosensor was applied to the quantification of lactate in real sweat samples.

2. Experimental

2.1. Reagents and solutions

Ethylene glycol, absolute ethanol, hydrogen peroxide 30% (w/v) and ortho-phosphoric acid 85% (w/w) were purchased from Scharlab (Sentmenat, Spain). Sodium L-lactate, poly(diallyldimethyl ammonium chloride) (PDDA) solution 20% (w/v) in water (Mw 100,000–200,000), chloroplatinic acid hexahydrate and the other chemicals were purchased from Sigma-Aldrich (Madrid, Spain) and used as received. Carbon nanofibers were kindly supplied by Showa Denko (Tokyo, Japan). L-Lactate oxidase (LOx) from *Pediococcus sp* was purchased from Sorachim S.A (Lausanne, Switzerland). LOx stock solution 1 U/μl was prepared in 0.1 M phosphate buffer pH 7.0 and aliquots of 20 μl were frozen until used. Other LOx solutions were prepared by dilution of thawed aliquots with 0.1 M phosphate buffer pH 7.0. The lactate stock solutions were prepared in 0.1 M phosphate buffer and 0.05 M NaCl pH 7.0 (PBS). H_2O_2 solutions were freshly prepared in PBS before each study, to avoid changes in the peroxide concentration by decomposition. All solutions were prepared with ultra pure water.

2.2. Apparatus and material

Electrochemical measurements were carried out with an ECO Chemie Autolab PGSTAT 128N potentiostat–galvanostat (KM Utrecht, The Netherlands), using the software package NOVA 1.9. Screen printed carbon electrodes (SPCEs) and edge-connector were produced at IK4-CIDETEC facilities. The configuration of the SPCEs was three-electrode printed on a plastic substrate. The electrodes were Ag/AgCl (pseudoreference electrode) and carbon (working and counter electrodes). An insulating layer served to delimit the working area (∅=4.4 mm) and electric contacts. All potentials reported here refer to this Ag/AgCl pseudoreference electrode. Scanning electron microscopy with energy dispersive spectroscopy module (SEM) JEOL JSM-5500LV (Tokyo, Japan), transmission electron microscopy (TEM) Tecnai 12 Bio Twin (Oregon, USA) and thermogravimetric balance model Q500-TGA TA Instruments (Delaware, USA) were used for the PtNp-CNF characterisation. Thieme 110E screen printing machine from Thieme GmbH & Co (Teningen, Germany), Lactate Scout analyser and Lactate Scout test strip from SensLab GmbH (Leipzig, Germany), Ultrapure Water Synthesis A10 from Millipore (Darmstadt, Germany), oven UNE 200 from Memmert (Winsconsin, USA), pHmeter GLP 2 from Crison (Barcelona, Spain), microfiltration vacuum system from Scharlab (Sentmenat, Spain), polytetrafluoroethylene membrane discs with mean pore size 0.22 μm from Millipore (Massachusetts, USA), microwave LG 700W-19L Touch Control from LG (Madrid, Spain) and ultrasonic bath Ultrasons HD-5L from J.P. Selecta (Barcelona, Spain) were also employed.

2.3. Deposition of PtNp on CNF

CNFs are highly graphitised nanofibers with diameters and lengths around 150 nm and 10 μm respectively. An oxidative treatment was carried out to improve the anchoring of the PtNp onto the CNFs. This procedure consisted of refluxing the CNFs in acidic media (1 M HNO_3, 0.5 M H_2SO_4, 120 °C, 6 h). Then, the CNFs were filtered on polytetrafluoroethylene membrane discs and washed with water. PtNp were deposited on CNFs by the microwave-assisted polyol method i.e. reduction of the metal precursor, H_2PtCl_6, by ethylene glycol in basic media (Chen et al., 2004). Finally, the PtNp-CNFs were filtered and washed again. The characterisation of PtNp-CNFs was carried out by SEM, TEM and TGA.

2.4. Preparation of the PtNp-CNFs-PDDA dispersions

PtNp-CNFs were weighed in a glass vial and suspended in 0.5% PDDA (w/v) solution for a final concentration of 0.5 mg/ml. The suspension was immersed in the ultrasound bath until a stable and homogeneous dispersion was achieved (around 1 h). Other PtNp-CNF-PDDA dispersions were prepared in the same way.

2.5. Preparation of the lactate biosensor

The electrode modification was carried out in several steps. First, 1.5 μl 30% EtOH (v/v) was uniformly spread on the electrode surface. Subsequently, 4 μl of PtNp-CNFs-PDDA was deposited and dried at room temperature (PtNp-CNFs-PDDA/SPCE). In the next step, 1.5 μl 30% EtOH (v/v) was uniformly spread on the PtNp-CNFs-PDDA/SPCE and 3 μl 0.33 U/μl LOx was subsequently added and left at room temperature for 2 h (LOx/PtNp-CNFs-PDDA/SPCE).

2.6. Analytical signal recording

The electrochemical measurements were performed by covering the three electrodes of the biosensor with 90 μl of the corresponding solution. Data were obtained from the chronoamperograms recorded at 0.5 V during 60 s. One sensor was used for each measurement.

2.7. Study of thermal degradation

Three batches of LOx/PtNp-CNFs-PDDA/SPCE were prepared and stored at 105, 115 and 125 °C respectively. The initial response for each batch was determined as the average current of five biosensors. The other biosensors of the batch were checked up at different incubation times (3 electrodes per point). All measurements were carried out with 1 mM lactate in PBS solution at room temperature.

2.8. Real sample measurements

Human sweat samples were obtained in a sport-training test. The subject ran on a treadmill for seven sets of increasing intensity. The speed of the treadmill was used to modify the heart rate of the subject. Each set was 4 min and was followed by a short rest period (15 s). The blood and sweat samples were collected from the fingers and forehead respectively during the breaks. The blood samples were analysed in situ while the sweat samples were kept at 4 °C. Afterwards, the sweat samples were diluted 1:25 with PBS before the analysis.

3. Results and discussion

3.1. Characterisation of the PtNp-CNFs

PtNp-CNFs were characterised by TEM (Fig. 1a) and SEM (Fig. 1b). The CNFs are tubelike with a mean diameter of 100–150 nm. The presence of walls inside the CNFs is evidenced by the light stripes along the central axis in Fig. 1a while the black points are PtNps. The distribution of these nanoparticles is not homogeneous and they are grouped at random places (Fig. 1b). The analysis of the TEM pictures provided a narrow gaussian distribution of diameters with the maximum value at 3.4 nm. These characteristics are usual for the nanoparticle synthesised by the polyol method where the ethylene glycol acts as reducing and dispersing agent. Thermogravimetric and EDX analysis were used to calculate the load of platinum in the PtNp-CNF. Both methods indicated around 17% Pt (w/w) (data not shown).

3.2. Optimisation of the PtNp-CNF-PDDA film

The oxidative treatment of the CNFs enhanced the adhesion of the PtNp but it was not effective in order to improve their solubility in water media. Hence, polymer wrapping was considered since homogeneous dispersion of nanomaterials had been reported using this simple and effective method (Merkoci et al., 2005). For this purpose, PDDA was chosen due to its polycationic nature, which induces positive charges on the PtNp-CNFs, facilitating both their dispersion in aqueous media and the retention of the enzyme by electrostatic attraction at neutral pH. Nevertheless, excessive amounts of nanomaterials and polymers can be against of the analytical performance (Lamas-Ardisana et al., 2008), so the composition of the PtNp-CNF-PDDA film on SPCEs was optimised for the amperometric detection of the hydrogen peroxide. Fig. 2 presents the amperometric currents (after the background subtraction) for 1 mM H_2O_2 in PBS solutions using SPCEs modified with different PtNp-CNF-PDDA films. On one hand, coatings obtained with PDDA solutions above 0.5% presented a progressive decrease in the signal-background ratio i.e. the enhancement of the PDDA resulted in lower peroxide currents and higher capacitive currents. SPCEs modified with films from 0.25 or 0.5% PDDA solutions provided quite similar signals. On the other hand, the effect of the PtNp-CNFs was apparently related to the PDDA. The lower the PDDA concentration, the lower the amount of PtNp-CNFs required to achieve the maximum current value was. For example, films from 0.25% PDDA solutions only required a concentration of 0.5 mg/ml PtNp-CNFs to reach the highest signal while films from 4% PDDA solution needed 1 mg/ml PtNp-CNFs or higher. Therefore, the effects of PDDA and PtNp-CNFs are opposite. This tendency could be related to PtNp blocking by PDDA which hinders the access of H_2O_2 to the catalytic centres. Hence, having considered the values of signals, backgrounds and reproducibility, a solution containing 0.5% PDDA and 0.5 mg/ml PtNp-CNFs was chosen as optimal for further studies.

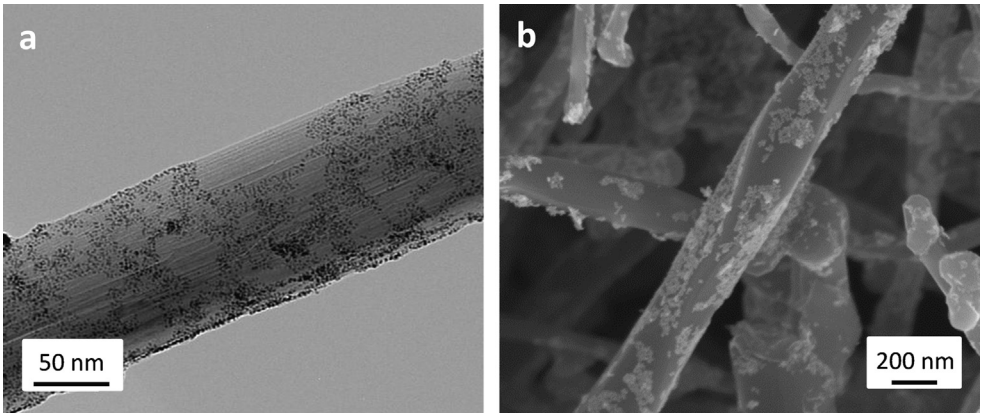

Fig. 1. TEM (a) and SEM (b) micrographs of the PtNp-CNFs.

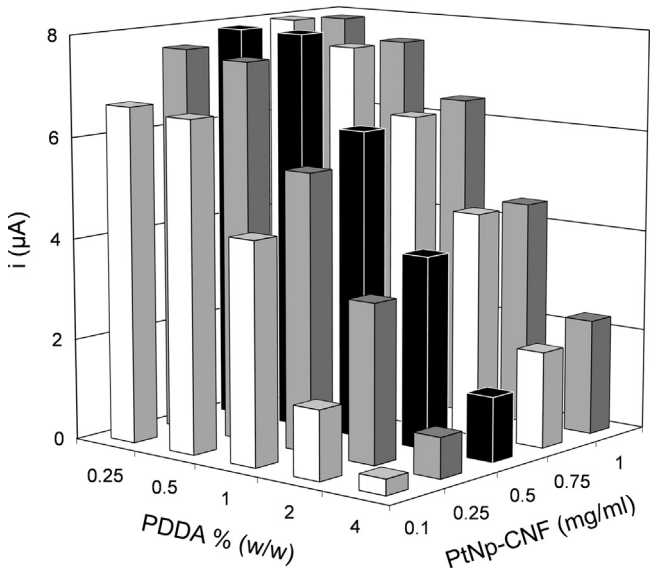

Fig. 2. Amperometric currents for 1 mM H_2O_2 in PBS solution using SPCEs modified with different PtNp-CNF-PDDA films. E=0.5 V and t=60 s. Background currents were subtracted in each case. Standard deviations are omitted for clarity (RSD < 7%; n=5).

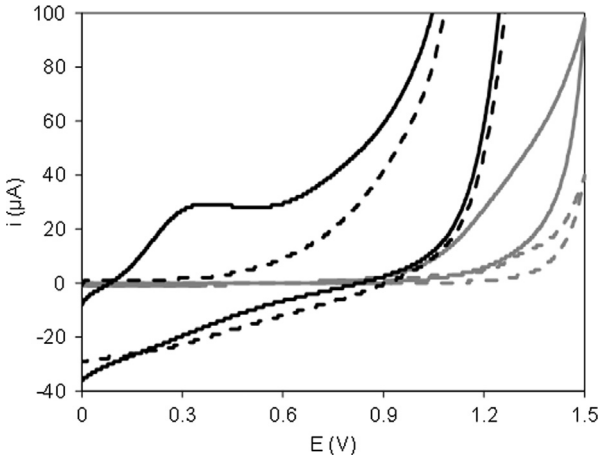

Fig. 3. Cyclic voltammograms of the PtNp-CNF-PDDA/SPCE (black lines) and bare SPCE (grey lines) in PBS (dash lines) containing 1 mM H_2O_2 (solid lines). Scan rate: 100 mV/s.

3.3. Electrocatalytic activity of PtNp-CNF-PDDA/SPCEs

Fig. 3 shows the cyclic voltammograms (CVs) obtained for PtNp-CNF-PDDA/SPCE and bare SPCE in the absence and presence of 1 mM H_2O_2. As illustrated, upon the addition of H_2O_2 on the PtNp-CNF-PDDA/SPCEs, the increase of the anodic current with respect to the background could be observed above 0.05 V and an oxidation peak was well defined around 0.3 V. The oxidation at bare SPCEs could be observed above 0.9 V although this process overlapped with water oxidation above 1.0 V. These CVs demonstrate that PtNp-CNF-PDDA films exhibit high electrocatalytic activity towards H_2O_2 oxidation. In order to confirm this property, control experiments were carried out with CNF-PDDA/SPCEs and PDDA/SPCEs (Fig. S1). H_2O_2 oxidation signals were almost equal in both cases. The shapes of these CVs were quite similar to those obtained at bare SPCE although the potentials shifted 0.5 V in the cathodic direction and the background currents increased substantially. These results indicate that the electrocatalytic efficiency could be attributed to PtNp in the PtNp-CNF-PDDA films.

3.4. Amperometric determination of H_2O_2 at PtNp-CNF-PDDA/SPCE

The PtNp-CNF-PDDA/SPCEs are attractive sensors for the amperometric detection of H_2O_2 taking into account their electrocatalytic properties and simple fabrication. The best performance for this application requires optimisation of the applied potential. Hence signals for 1 mM H_2O_2 in PBS solution were registered at different potentials. The anodic current increased almost lineally above 0.05 V and levelled off around 0.4 V (Fig. S2). Insignificant changes of the background currents were detected in the same experiment without H_2O_2. Therefore, 0.5 V was chosen as the optimum value, ensuring that the applied potential was kept inside the current plateau zone. The subsequent calibration for H_2O_2 in PBS solution indicated that the PtNp-CNF-PDDA/SPCEs have a wide linear range (2.5–10,000 μM), low limit of detection (2.4 μM; based on S/N=3) and good sensitivity (46.7 mA/M cm^2) (Fig. S3). The reproducibility was 5.3%, calculated from ten signals for 1 mM H_2O_2 in PBS.

3.5. Amperometric determination of lactate at LOx/PtNp-CNF-PDDA/SPCE

The PtNp-CNF-PDDA/SPCEs were used as platforms for the construction of lactate biosensors. Firstly, the amount of lactate oxidase (LOx) was optimised to achieve the highest sensitivity (Fig. S4). Biosensors with different amounts of LOx (between 0.25 and 3 U per electrode) were prepared and measurements for solutions of 0.25–1.5 mM lactate in PBS were carried out. The slopes were determined from the linear ranges of the calibration plots. The relationship between the slopes and LOx units presented an asymmetric gaussian shape. Initially, there was a large increase in the slopes for small amounts of LOx. Above 0.5 U per electrode, the enhancement of the slope was moderated and the maximum value was observed at 1 U per electrode. Higher enzymatic loads resulted in a progressive loss of sensitivity. Therefore, 1 U per electrode was chosen as optimal value (LOx/PtNp-CNF-PDDA/SPCEs). On the other hand, the effect of pH and detection potential were also studied. Negligible changes were observed for signals registered at pH between 5.5 and 8.5. The effect of the applied potential for the lactate determination at LOx/PtNp-CNF-PDDA/SPCEs was similar to the one previously described for the amperometric detection of H_2O_2 at PtNp-CNF-PDDA/SPCEs. In this case, the current plateau was slightly shifted to higher potentials i.e. above 0.5 V (Fig. S5). This could be related to the slower electron transfer kinetics as a consequence of the enzyme adsorption into the electrode surface. Thus, 0.5 V was chosen as detection potential.

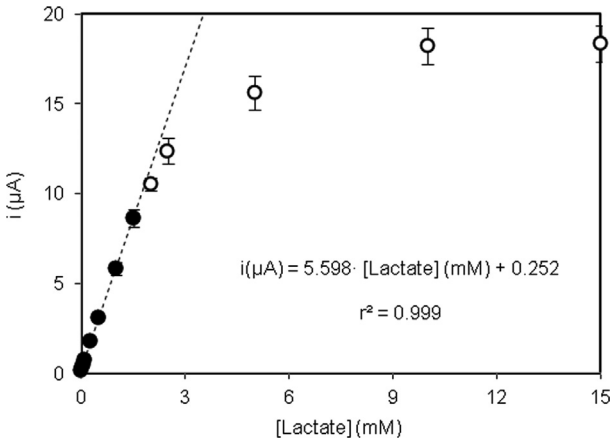

Fig. 4. Calibration curve of lactate with LOx/PtNp-CNF-PDDA/SPCEs. E=0.5 V and t=60 s. Black circles indicate the linear range. Data are given as average for three electrodes.

Fig. 4 shows the calibration curve obtained for the optimised LOx/PtNp-CNF-PDDA/SPCE. The biosensor showed Michaelis–Menten kinetics. Using the Lineweaver–Burk linearization, the Michaelis–Menten constant was determined as 1.6 mM, which is comparable to or lower than corresponding values observed in other reports (16.7 mM, Wang et al., 2006; 2.25 mM, Sung and Bae, 2006 or 2.6 mM, Ges and Baudenbacher, 2010). A linear relationship between current and lactate concentration was obtained in the range of 25–1500 μM with excellent coefficient of determination (r^2=0.999) and sensitivity of 36.8 mA/M cm^2. The limit of detection was 11.1 μM (based on S/N=3) and the reproducibility (RSD, n=10) was 5.8%, calculated from signals of lactate 1 mM in PBS solution. The analytical performance of the LOx/PtNp-CNF-PDDA/SPCEs is comparable, in terms of linear range and detection limits, to other biosensors based on drop (non-stirring) measurements (Table S1). The sensitivity of the LOx/PtNp-CNF-PDDA/SPCEs is clearly superior under these conditions (Perez et al., 2012; Rawson et al., 2009; Shimomura et al., 2012), although higher sensitivities have been published for lactate biosensors in stirring solutions (Male et al., 2007; Perez and Fabregas, 2012; We et al., 2003). Inks containing platinum on carbon have also been proposed in lactate biosensors but low sensitivities and/or small linear ranges were reported (Albareda-Sirvent and Hart, 2002; Collier et al., 1996). Finally, multiwall carbon nanotubes decorated with PtNp have demonstrated important benefits for lactate biosensors, particularly when low limits of detections are required (Male et al., 2007).

The specificity of the biosensor was studied considering the detection of lactate in sweat. Potentially interfering compounds were selected from the standard constituents of the human sweat (Faridnia et al., 1993; Guilbault et al., 1995; Harvey et al., 2010). In order to obtain a realistic evaluation of the specificity, the concentrations were at least twice their maximum values in sweat i.e. amino acids (Tyr, Val, Arg, His, Lys, Leu, and Thr), uric acid, thiamine, ascorbic acid, paracetamol (0.1 mM), glucose, acetylsalicylic (5 mM), urea (15 mM) and glycine (15 mM). The amino acids were prepared together in a unique solution whereas the other interfering compounds were individually prepared. All solutions were prepared in PBS and contained 1 mM lactate. The signals obtained for lactate solutions with and without interfering compounds were comparable and the percentage error was lower than 5% for each case (Fig. S6). Hence, LOx/PtNp-CNF-PDDA/SPCEs have good specificity for the detection of lactate in human sweat. Nevertheless, it should be noticed that significant interference was observed for higher levels of uric acid, paracetamol and, specially, ascorbic acid. The origin of these interferences could be related to the direct electrochemical oxidation of these compounds at the conditions used for the detection.

3.6. Storage stability of the biosensors

LOx/PtNp-CNF-PDDA/SPCEs were prepared and kept in a closed light-protected container until their use. The biosensors stored at room temperature were stable at least 6 months without significant loss of sensitivity. Then, an accelerated degradation protocol was used to predict the life of the biosensors in a short period of time (McAteer et al., 1999). First order kinetics and no intermediates are assumed in the deactivation process of this model. A simple Arrhenius type plot provides a basis for the deactivation profiles

$$\ln(i/i_0) = -K_T t \quad (1)$$

where t is the storage time in days, i_0 is the response of the biosensors at the initial stage, i is the signal after t incubation days in the oven and K_T is the constant of deactivation for a particular temperature. The evolution of the signals at different temperatures is presented in Fig. 5a. The biosensors presented high thermal stability and temperatures above 100 °C were required for the fast deactivation of the biosensors. Thus, 50% of the biosensor response was maintained after four days at 105 °C. The experimental values of the K_T were determined from Eq. (1) and the slopes of the equations obtained by simple linear regression for each temperature. Then, plotting the natural log of these K_T against the reciprocal of the temperature resulted in a linear relationship (Fig. 5b). This curve allowed the estimation of the K_T at different temperatures and, consequently, the storage stability of the biosensors could be predicted using Eq. (1) again. Hence the forecast by this model is that 90% of the initial signal would be retained after 16 months at 25 °C. Although this data is a rough estimation of the long term stability of the developed sensors, it is valuable enough to underline that stability will not be a handicap for commercial applications.

3.7. Sweat analysis

A commercial device (Lactate Scout) was used to analyse the blood samples and the diluted sweat samples. Although this analyser is intended only for blood samples, it works for lactate in PBS with a small correction (Fig. S7). The concentrations of lactate in the diluted sweat samples were also determined by LOx/PtNp-CNF-PDDA/SPCEs. In this case, the data were interpolated using a calibration curve. The differences between the results from LOx/PtNp-CNF-PDDA/SPCEs and commercial analyser were lower than 4.8% for the lactate concentration in sweat samples (data not shown), which indicates the accuracy of the biosensors developed in this work.

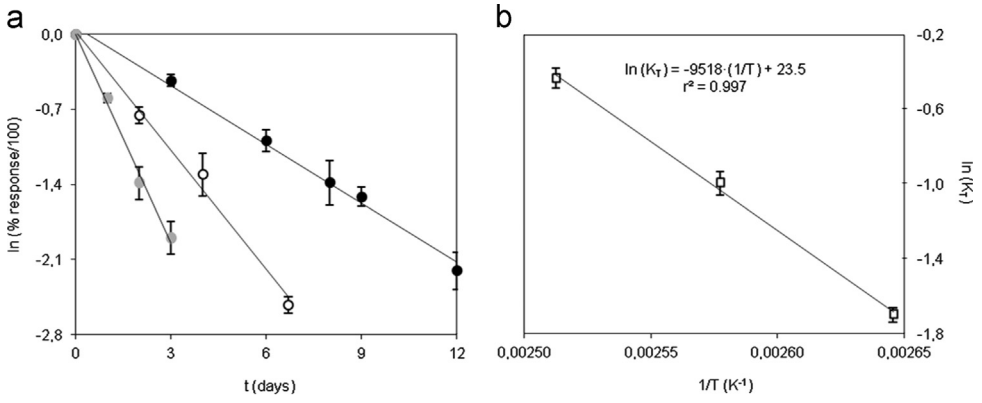

Fig. 5. (a) Semi-log plot of the biosensors deactivation at 105 °C (black circles), 115 °C (white circles) and 125 °C (grey circles), and (b) semi-log plot of deactivation constants vs temperature. Details in Section 2.7.

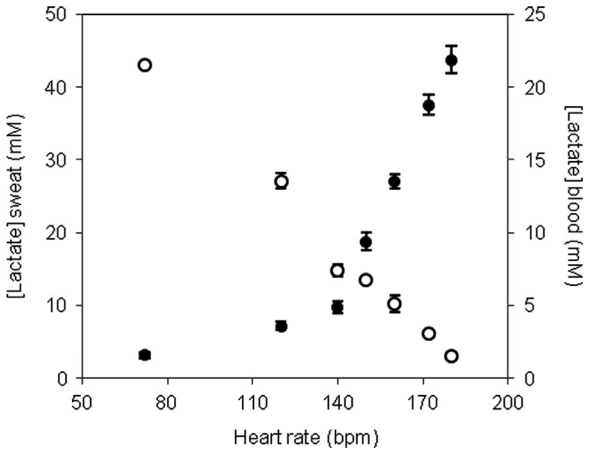

Fig. 6. Concentrations of lactate in sweat samples (white circles; analysed by LOx/PtNp-CNF-PDDA/SPCEs) and blood samples (black circles; analysed by Lactate Scout) at different heat rates. Data are the average of 3 signals. Details are shown in Section 2.

Fig. 6 summarises the results obtained for blood (by Lactate Scout) and sweat samples (by LOx/PtNp-CNF-PDDA/SPCEs). The blood lactate concentration showed the expected behaviour since the concentration increased with the exercise intensity. The lactate threshold was around 140 bpm based on the blood lactate curve. On the other hand, the sweat lactate concentrations presented an initially high concentration that decays with heart rate. These data agree with previous studies reported elsewhere (Fellmann et al., 1983). Although an increase of the sweat lactate concentration with the exercise intensity could be expected, there is still some controversy about this dependence (Derbyshire et al., 2012). For example, the rate of sweating has a marked effect and the lactate can be diluted when the sweating rate increases. This fact would explain the tendency of the sweat lactate in Fig. 6 since the perspiration rate of the subject increased notably during the test. Hence, the relationship between the lactate levels in blood and sweat has been widely questioned and our comparison supports this argument since absolutely opposing tendencies were observed.

4. Conclusions

PtNp-CNFs were successfully used for the amperometric detection of H_2O_2. The good performance can be related to a good dispersion of the platinum nanoparticles on a highly conducting CNF support and their electrocatalytic activity towards the H_2O_2 oxidation and reduction. On the other hand, dispersions of PtNp-GNF in aqueous media were achieved by wrapping method. The polycation PDDA showed great capacity for the stabilisation of PtNp-GNF dispersion and highly concentrated solutions were attained with low PDDA concentrations. Nonetheless the PtNp-CNF/PDDA ratio and the total amount of nanocomposite had to be optimised for the electrode modification since the amperometric detection of the H_2O_2 relies heavily on it. The optimised PDDA-PtNp-CNF/SPCE is a novel and suitable platform for lactate biosensors, which are obtained by LOx adsorption on top of them. The analytical performance of the biosensors is suitable for the determination of lactate in sweat and they exhibit high storage stability. The sensitivity of the biosensor was constant at room temperature for 6 months and 90% would remain after 16 months, based on a rough estimation of the thermal stability. Finally, lactate in real sweat samples was successfully determined with these biosensors. The results of our sport-test suggest that sweat lactate levels, while varying with the exercise intensity, follow the opposite trend to blood lactate levels. Therefore, these results reinforce that sweat lactate is not suitable to determine the lactate threshold.

Acknowledgements

The authors are grateful for the financial support received from the ENIAC JOINT UNDERTAKING – Nanoelectronics for Mobile Ambient Assisted Living (AAL) Systems Project Grant Agreement No. 12 02 28. P.J.L.A. acknowledges financial support from the DGI of MICINN (Torres Quevedo Program; ref: PTQ-10-03209). The authors do also want to acknowledge the technical collaboration of Eider Begiristain in this work.

Appendix A. Supporting information

Supplementary data associated with this article can be found in the online version at http://dx.doi.org/10.1016/j.bios.2014.01.047.

References

Albareda-Sirvent, M., Hart, A.L., 2002. Sens. Actuators B Chem. 87 (1), 73–81.
Andersen, S.M., Borghei, M., Lund, P., Elina, Y.-R., Pasanen, A., Kauppinen, E., Ruiz, V., Kauranen, P., Skou, E.M., 2013. Solid State Ion. 231, 94–101.
Andrzejewski, M., Chmura, J., Dybek, T., Pluta, B., 2012. Biol. Sport 29 (3), 185–191.
Artiss, J.D., Karcher, R.E., Cavanagh, K.T., Collins, S.L., Peterson, V.J., Varma, S., Zak, B., 2000. Am. J. Clin. Pathol. 114 (1), 139–143.
Avramescu, A., Andreescu, S., Noguer, T., Bala, C., Andreescu, D., Marty, J.L., 2002. Anal. Bioanal. Chem. 374 (1), 25–32.
Buckley, J.D., Bourdon, P.C., Woolford, S.M., 2003. J. Sci. Med. Sport 6 (4), 408–421.
Collier, W.A., Janssen, D., Hart, A.L., 1996. Biosens. Bioelectron. 11 (10), 1041–1049.
Chen, W., Cai, S., Ren, Q.-Q., Wen, W., Zhao, Y.-D., 2012. Analyst 137 (1), 49–58.
Chen, W.X., Lee, J.Y., Liu, Z.L., 2004. Mater. Lett. 58 (25), 3166–3169.
Chikae, M., Idegami, K., Kerman, K., Nagatani, N., Ishikawa, M., Takamura, Y., Tamiya, E., 2006. Electrochem. Commun. 8 (8), 1375–1380.
Derbyshire, P.J., Barr, H., Davis, F., Higson, S.P.J., 2012. J. Physiol. Sci. 62 (6), 429–440.
Fanjul-Bolado, P., Hernandez-Santos, D., Lamas-Ardisana, P.J., Martin-Pernia, A., Costa-Garcia, A., 2008. Electrochim. Acta 53 (10), 3635–3642.
Fanjul-Bolado, P., Queipo, P., Jose Lamas-Ardisana, P., Costa-Garcia, A., 2007. Talanta 74 (3), 427–433.
Faridnia, M.H., Palleschi, G., Lubrano, G.J., Guilbault, G.G., 1993. Anal. Chim. Acta 278 (1), 35–40.
Faude, O., Kindermann, W., Meyer, T., 2009. Sports Med. 39 (6), 469–490.
Fellmann, N., Grizard, G., Coudert, J., 1983. J. Appl. Physiol. 54 (2), 355–360.
Frost, M., Meyerhoff, M.E., 2006. Anal. Chem. 78 (21), 7370–7377.
Ges, I.A., Baudenbacher, F., 2010. Biosens. Bioelectron. 26 (2), 828–833.
Guilbault, G.G., Palleschi, G., Lubrano, G., 1995. Biosens. Bioelectron.10, 379–392.
Harvey, C.J., LeBouf, R.F., Stefaniak, A.B., 2010. Toxicol. In Vitro 24 (6), 1790–1796.
Huang, J., Li, J., Yang, Y., Wang, X., Wu, B., Anzai, J.-i., Osa, T., Chen, Q., 2008. Mater. Sci. Eng. C Biomim. Supramol. Syst. 28 (7), 1070–1075.
Huang, J.S., Liu, Y., You, T.Y., 2010. Anal. Methods 2 (3), 202–211.
Jia, W., Bandodkar, A.J., Valdes-Ramirez, G., Windmiller, J.R., Yang, Z., Ramirez, J., Chan, G., Wang, J., 2013. Anal. Chem. 85 (14), 6553–6560.
Lamas-Ardisana, P.J., Queipo, P., Fanjul-Bolado, P., Costa-García, A., 2008. Anal. Chim. Acta 615 (1), 30–38.
Liu, Y., Wang, D., Xu, L., Hou, H., You, T., 2011. Biosens. Bioelectron. 26 (11), 4585–4590.
Male, K.B., Hrapovic, S., Luong, J.H.T., 2007. Analyst 132 (12), 1254–1261.
McAteer, K., Simpson, C.E., Gibson, T.D., Gueguen, S., Boujtita, M., El Murr, N., 1999. J. Mol. Catal. B Enzym. 7 (1–4), 47–56.
Merkoci, A., Pumera, M., Llopis, X., Perez, B., del Valle, M., Alegret, S., 2005. TrAC Trends Anal. Chem. 24 (9), 826–838.
Perez, S., Fabregas, E., 2012. Analyst 137 (16), 3854–3861.
Perez, S., Sanchez, S., Fabregas, E., 2012. Electroanalysis 24 (4), 967–974.
Pfeiffer, D., Möller, B., Klimes, N., Szeponik, J., Fischer, S., 1997. Biosens. Bioelectron. 12 (6), 539–550.
Piano, M., Serban, S., Pittson, R., Drago, G.A., Hart, J.P., 2010. Talanta 82 (1), 34–37.
Polliack, A., Taylor, R., Bader, D., 1997. J. Rehabil. Res. Dev. 34 (3), 303–308.
Przybyt, M.g., Iciek, J., Papiewska, A., Biernasiak, J., 2010. J. Food Eng. 99 (4), 485–490.
Rawson, F.J., Purcell, W.M., Xu, J., Pemberton, R.M., Fielden, P.R., Biddle, N., Hart, J.P., 2009. Talanta 77 (3), 1149–1154.
Saunders, A.C., Feldman, H.A., Correia, C.E., Weinstein, D.A., 2005. J. Inherit. Metab. Dis. 28 (5), 695–701.
Shimomura, T., Sumiya, T., Ono, M., Ito, T., Hanaoka, T.-a., 2012. Anal. Chim. Acta 714, 114–120.
Simonides, W.S., Zaremba, R., van Hardeveld, C., van der Laarse, W.J., 1988. Anal. Biochem. 169 (2), 268–273.

Sung, W.J., Bae, Y.H., 2006. Sens. Actuators B Chem. 114 (1), 164–169.
Thomas, N., Laehdesmaeki, I., Parviz, B.A., 2012. Sens. Actuators B Chem. 162 (1), 128–134.
Tudorache, M., Bala, C., 2007. Anal. Bioanal. Chem. 388 (3), 565–578.
Wang, D., Liu, Y., Huang, J., You, T., 2012. J. Colloid Interface Sci. 367, 199–203.
Wang, J., Musameh, M., Lin, Y.H., 2003. J. Am. Chem. Soc. 125 (9), 2408–2409.
Wang, K., Xu, J.-J., Chen, H.-Y., 2006. Sens. Actuators B Chem. 114 (2), 1052–1058.
Wang, Y.T., Yu, L., Wang, J., Lou, L., Du, W.J., Zhu, Z.Q., Peng, H., Zhu, J.Z., 2011. J. Electroanal. Chem. 661 (1), 8–12.
We, X., Zhang, M.G., Gorski, W., 2003. Anal. Chem. 75 (9), 2060–2064.
Xiao, Y., Li, C.M., 2008. Electroanalysis 20 (6), 648–662.
Xu, B., Ye, M.-L., Yu, Y.-X., Zhang, W.-D., 2010a. Anal. Chim. Acta 674 (1), 20–26.
Xu, X., Jiang, S., Hu, Z., Liu, S., 2010b. ACS Nano 4 (7), 4292–4298.